3.3 GENERATING RIVER DISCHARGE ESTIMATES FOR THE BAY OF BENGAL USING NASA'S LAND INFORMATION SYSTEM

JOHN E. M. BROWN*
University of Miami/Rosenstiel School of Marine and Atmospheric Science, Miami, Florida

1. Introduction

Although the land drainage area of the Indian Ocean is rather small – the west coast of Africa, Madagascar, the coastal strip of western Australia, Sumatra, Java, and the Indian and Indochinese Sub-Continent – the influence of the Asian rivers is amplified by the monsoonal climate. The summer floodwaters of the Ganges and Brahmaputra rivers discharging into Bay of Bengal plus the Irrawaddy and Salween rivers emptying into the Andaman Sea combine to influence the salinity of the surface waters over thousands of kilometers offshore (Tomczak and Godfrey, 1994). This fact was confirmed during the summer 2001 Bay of Bengal Ocean Process Studies cruise, where the copious amounts of rainfall and river runoff freshened the upper 30 m of the Bay by 3-7 psu compared to the central Arabian Sea (Prasanna Kumar et al. 2002).

In the hydrological research community the Bay of Bengal and Andaman Sea have not been studied as much as other regions. While global climate models (GCM's) have produced on continental scale estimates for this region (e.g. Miller et al. 1994; Lau et al. 1996; Bosilovich et al. 1999; etc.), there has been little, if any, basin scale modeling studies conducted.

The role of river influx, especially that from the Ganges/Brahmaputra rivers, in the dynamics of coastal currents in the Bay of Bengal is not known.

2. Land Surface Modeling

Land surface modeling seeks to predict the terrestrial water, energy, and biogeochemical processes by solving the governing equations of the soil-vegetation-snowpack medium (Kumar et al. 2006). The land surface and atmosphere are coupled to each other over a variety of time scales through the exchanges of water, energy, and carbon. An accurate representation of land surface processes is critical for improving models of the boundary layer and land-atmosphere coupling at all spatial and temporal scales and over heterogeneous domains. Long term descriptions of land use and fluxes also enable the accurate assessments of climate characteristics. In addition to the impact on the atmosphere, predicting land surface processes is also critical for many real-world applications such as ecosystem modeling, agricultural forecasting, mobility assessment, and water resources prediction and management (Kumar et al. 2006).

Our interest here is in using the land surface models within NASA's Land Information System (LIS) to generate surface runoff from rainfall estimates with the ultimate goal of producing river discharge estimates.

Corresponding author address: John E. M. Brown, University of Miami/RSMAS, MPO Division, 4600 Rickenbacker Causeway, Miami, FL 33149;
Email: jemb@rsmas.miami.edu

3. NASA's Land Information System

The Land Information System (LIS) was developed (and currently operated) by the Hydrological Sciences Branch (Code 613.4) at NASA's Goddard Space Flight Center (GSFC) (Kumar et al. 2006). LIS is a high performance land surface modeling and data assimilation system, based on GSFC's Land Data Assimilation Systems (LDAS) (Rodell et al. 2004). One of the LIS objectives is to formulate a parameterization of runoff-generation processes more physically based than that of conceptual models, while achieving a computational efficiency that allows for its operational use in midsize basins. Figure (1) shows a schematic of LIS.

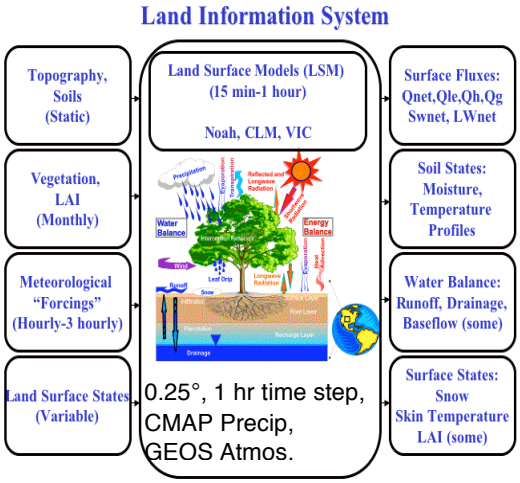

Fig. 1 Schematic showing the Land Information System modeling concept. Output from the surface models translates to hydrological variables such as soil moisture, surface runoff, etc. Model run conducted for 2001 and 2002 at 0.25° resolution, 1hour time step, NOAH land surface model, CMAP precipitation forcing, and GEOS atmospheric forcing.

The land surface models simulate soil moisture variations, evapo-transpiration, and runoff on single grid cells using bio-physical data sets that include climatic drivers, vegetation, and soil properties. The state variables are determined by interactions among time-varying precipitation, potential evapo-transpiration, and soil water content.

4. River Routing

In order to generate a streamflow hydrograph for comparison with observations it is necessary to route the runoff from each model grid cell to the basin outlet using a post-processor routing model. Preparation for running the routing model requires development of a routing network for the grid cells, describing the flow paths from cell-to-cell, in addition to several other input files (VIC operation overview, 2002). Often a routing model works on longer time steps than the land surface model (i.e. using daily runoff versus hourly LSM output) so that the fluxes created by the LSM need to be aggregated prior to routing the flows.

Due to its availability to the scientific community we focus on the using the VIC River Routing Model developed by Dag Lohmann (Lohmann et al. 1996; Lohmann et al. 1998a; Lohmann et al. 1998b). It calculates the timing of the runoff reaching the outlet of a grid box, as well as the transport of the water through the river network. It can be coupled directly into a land surface scheme, thus adding a state variable "surface water" to that LSM, or it can be used off-line (as in this study) from the LSM with no further feedback.

It is assumed that water can leave a grid cell only in one of its eight neighboring grid cells, given by the river flow direction mask. Each grid cell can also function as the sink of runoff from its upstream area. Both internal grid cell processes and river routing time delays are represented using linear, time invariant and causal models (Lohmann et al. 1998a) that are represented by non-negative impulse-response functions. Figure 2 is a schematic of the VIC river routing model.

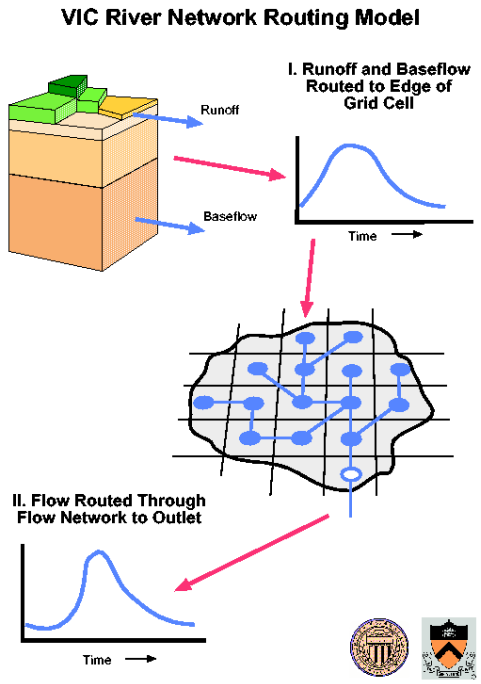

Fig. 2 The VIC river routing model transports grid cell surface runoff and baseflow produce by the VIC land surface model (or in our case by Noah from LIS) within each grid cell to the outlet of that grid cell then into the river system. Internal cell routing uses a Unit Hydrograph approach. Channel routing uses the linearized Saint-Venant equation. The river routing model assumes all runoff exits a cell in a single flow direction. Source – Univ. of Washington.

The equation used for the transport within the river is the linearized St.Venant Equation (Mesa and Mifflin, 1986; Fread, 1993):

$$\partial Q/\partial t = D \bullet \partial^2 Q/\partial x^2 - C \bullet \partial Q/\partial x \qquad (1)$$

where Q is the discharge, D a dispersion of diffusion coefficient, and C the velocity. The parameters C and D can be found from measurements or by rough estimation from geographical data of the riverbed. Wave velocity C and diffusivity D must be seen as effective parameters, as there is often more than one river in a grid box or because of human-made changes.

Finally, one ends up with a single value of C and D for every grid box, which reflects the main characteristics of the water transport in a river. Equation (1) can be solved with convolution integrals:

$$Q(x,t) = \int_0^t U(t-s)h(x,s)ds \qquad (2)$$

where

$$h(x,t) = \{x/[2t(\pi tD)^{1/2}]\} * \exp\{-(Ct-x)^2/4Dt\} \qquad (3)$$

is Green's function (or impulse response function) of equation (2) with boundary values and initial condition $h(x,0) = 0$ for $x > 0$ and $h(0,t) = \delta(t)$ for $t \geq 0$.

Due to its linearity and the numerical stability of this solution the influence of dams, weirs, and water use can easily be implemented into the scheme at every node (Lohmann et al. 1996).

The Appendix describes the method used to calculate the wave velocity, C. Diffusivity was set to D = 800 m^2/s following the recommendation of the University of Washington VIC online documentation[1].

[1] http://www.hydro.washington.edu/

5. Artificial River Network

River runoff generated in the real world must be routed through a natural network of water flow paths, such as creeks, brooks, tributaries, and major river channels. These paths must be accurately sorted to generate a dataset of basin-scale water channels (Oki and Sud, 1998).

In this study we use the Simulated Topological Network at 30-minute (~50 km^2 at the equator) resolution (STN-30), developed at the University of New Hampshire (Vörömarty et al. 2000). STN-30 organizes the ~60,000 half degree continental land cells into 6152 river basins with sizes ranging from a few hundred km^2 to 5.8×10^6 km^2. Out of the 6152 river basins represented in STN-30, 1123 have more than 10,000 km^2 in catchment area (approximately 5 cells) that could be considered the smallest catchment area that a 50 km resolution network can potentially represent. Experience at UNH has shown that, in general, river basins with catchment areas ≥ 25,000 km^2 can be accurately represented by STN-30 (Fekete et al. 2000).

STN-30 also contains a set of derived data sets that make the representation of river systems more comprehensive. Every river segment (grid cell with flow direction) has a set of attributes such as basin identifier, upstream catchment area, main stem length, distance to receiving end-point downstream, Strahler's stream order (Strahler, 1964), etc. According to Fekete et al. (2000) STN-30 is suitable for monthly flow simulations. Figure 3 shows the STN-30 network for the area of study.

Each grid point in STN-30 was idealized to have only one outflow direction with reference to its eight neighboring grid points: N, NE, E, SE, S, SW, W, and NW.

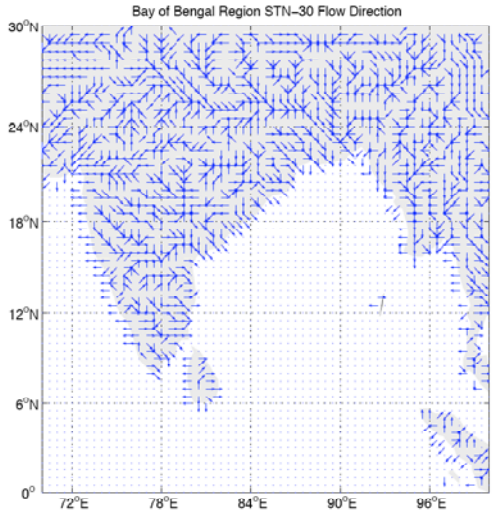

Fig. 3 – Flow direction for the STN-30 0.5° river network for the Bay of Bengal area of study.

This is a so-called "D8" scheme and its disadvantages are discussed in Costa-Cabral and Burges (1994). They show that statistical or partial treatment of river channel network, in which each grid may have two or more outflow grids, may be more realistic in some cases, particularly for regions with complicated boundaries. For the global domain, however, the "D8" format amply represents the area size adequately and relates to the lateral flow directions realistically.

The hydrological flow modeling method (Chorowicz, 1992) is used for most D8-type river channel networks. The outflow direction is pointed toward the lowest land point of the eight neighboring grids, provided the new outflow point is lower than the originating point. At first glance it would appear that the direction toward the steepest slope should be the obvious choice but considering that there could be meandering and

unevenness within the subgrid scale, it is assumed that the water will somehow find a way to reach the lowest level.

6. Model Set-Up and Experimental Design

For this study LIS was configured to start from a "cold start" using climatology and default values. We chose the NOAH land surface model (Ek et al. 2003) since this was the model given in an example configuration in the LIS User's Guide as well as being actively used at NASA GSFC during the 2005 NASA Graduate Student Summer Program. Atmospheric forcing was provided by NASA's finite volume Global Numerical Weather Model (GEOS) (Pfaendtner et al. 1995). Precipitation forcing was provided by NOAA's CMAP (Xie and Arkin, 1996). LIS was run on hourly time steps with daily output for the period December 2000 through January 2003.

Since long-term, consistent forcing data sets were not available for spinning up LIS toward perfect initial conditions and due to the limited computational resources, we chose to initialize our model by looping repeatedly through the model run period. In our case this process was repeated five times. Given the limitations just mentioned above, this is perhaps the most common spin-up method in practice today (Rodell et al. 2005). When the land surface states and/or fluxes equilibrate (cease to vary appreciably from year-to-year), the spin-up is considered complete and the experimental simulation is allowed to commence. In the Project for Inter-comparison of Land Surface Parameterization Schemes (PILPS) spin-up time was defined as the number of yearly integrations necessary to yield changes in annual mean latent heat and sensible heat fluxes that were less than 0.1 W/m^2. Based on this definition, Yang et al. (1995) found that spin-up times for 22 PILPS Phase 1 LSMs running on a single point and starting from a middling moisture condition ranged from 2 to 10 years for a tropical forest and from 2 to 15 years for a mid-latitude grassland site. Rodell et al. (2005) evaluated various methods of initializing land surface models and found that humid regions spun up much more quickly than arid regions. Thus our own spin-up procedure may not have reached an optimum end state.

However, finding the best initial state was not the focus of this research and after discussions with the NASA LIS project team (Yudong Tian, pers. comm. 2006) these concerns were judged to have a minimal impact since in the experience of the NASA LIS project team a spin-up of 5 years worked well for this type of application.

Model performance is analyzed for the 2001-2002 calendar years looking at the combined Ganges-Brahmaputra (GB) basin as the first case. We test the hypothesis on whether coupling a river routing scheme is beneficial or not. In Appendix A we show that the travel times for most river basins in the study area were less than 30 days. Thus, one could make the argument that river routing is not that necessary when dealing with monthly time scales of interest. All one would need to do is total the surface runoff in a month and use that as a substitute parameter for river discharge (C. Peters-Lidard, pers. comm. 2005). These results are presented as part of the "no routing" case where monthly surface runoff values (Qs) are listed in Table 1 for the GB river basin.

After the GB river basin results are presented we turn our attention to the other major river basins draining into the Bay of Bengal, specifically the Irrawaddy, Godavari, Krishna, and Salween.

In the STN-30 network the Ganges and Brahmaputra river basins are one large basin (Figure 4).

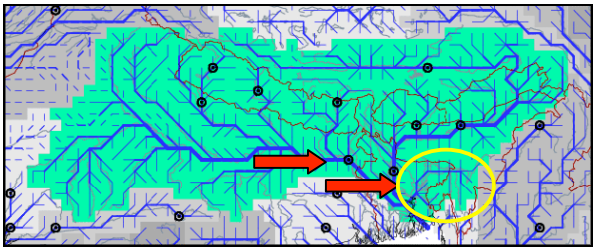

Fig. 4 – STN-30 Ganges/Brahmaputra combined river basin. The two GRDC river gauge stations used in this study are marked by the red arrows – Farakka, India (above left) and Bahadurabad, Bangladesh (below right). The Meghna river network is shown within the yellow circle. The flow from the Meghna river is not accounted for by any gauging station. Source - University of New Hampshire

We extract these areas from the larger network and form one Ganges/Brahmaputra (GB) watershed. We identify the boundary of the GB watershed and determine whether the LIS surface runoff (Qs) and subsurface baseflow (Qsb) values are within the boundary. All Qs and Qsb values within the GB boundary are output as daily and monthly averages. The LIS Qs and Qsb output values are given in mass flux terms of kg m^2/s. This standard conforms to the ALMA (Assistance for Land-surface Modeling Activities) data exchange convention.[2]

To make comparisons with observed data, we need to convert the output to river discharge values in m^3/s. In order to convert the surface runoff, R (kg m^2/s) to the discharge at the river outlet, Q (m^3/s), we need the corresponding drainage area, *A* (km^2) as well as the specific volume of water, ρ^{-1} (m^3/1000 kg). The conversion equation becomes:

$$Q = R \times (A \times 10^3) \times \rho^{-1} \quad (4)$$

Using the STN-30 area for both stations – 941,428 km^2 for Farakka and 554,542 km^2 for Bahadurabad, we have an estimate of 1,495,970 km^2 for the total catchment area. Inputting these values into equation (4) gives us our river discharge estimates in m^3/s. Since the LIS Qs and Qsb output values are at a 0.25° resolution they have to be averaged for their corresponding 0.5° STN-30 grid cells. Each grid cell within the GB boundary has its own STN-30 cell area attribute.

Climatology data came from the University of New Hampshire/Global River Data Center (UNH/GRDC) composite runoff fields version 1.0 (Fekete et al. 2000).[3] We use the station Farakka, India to represent the Ganges outlet and the station Bahadurabad, Bangaldesh for the Brahmaputra outlet before the confluence of these rivers discharge into the Bay of Bengal. A statistical summary for each station can be found at the website below.

River discharge observation data came from Dr. Peter Webster's Climate Forecast Applications in Bangladesh (CFAB) group at the Georgia

[2] More about ALMA is available online at: http://www.lmd.jussieu.fr/~polcher/ALMA/

[3] UNH/GRDC composite runoff fields v1.0 available online at: http://www.grdc.sr.unh.edu/

Institute of Technology (GT) [4] and their partner, the Bangladesh Flood Forecasting and Warning Center[5] (FFWC). The data are from two stations – Hardinge Bridge, Bangladesh and Bahadurabad, Bangladesh. Hardinge Bridge (24.07°N 089.03°E) is located about ~80 km downstream from the Farakka Barrage (25.00°N 087.92°E) (T. Hopson, pers. comm. 2006).

For the purposes of this study, we shall treat the Hardinge Bridge data as if it came from Farakka, India. This convention will be used in labeling graphs, etc. Discharge measurements of Q (m^3/s) were taken at the following local times: 0600, 0900, 1200, 1500 and 1800. These measurements were then averaged into daily, 8-day weekly, and monthly values for our analysis.

Data are available for 2001 (Hardinge Bridge is missing data for March, 2001) and 2002. We replace the March missing data by taking the February 28 daily value and reducing linearly to the April 1st daily value. This is consistent with the March, 2001 observations from Bahadurabad. Figure 5 shows the locations of the FFWC station network.

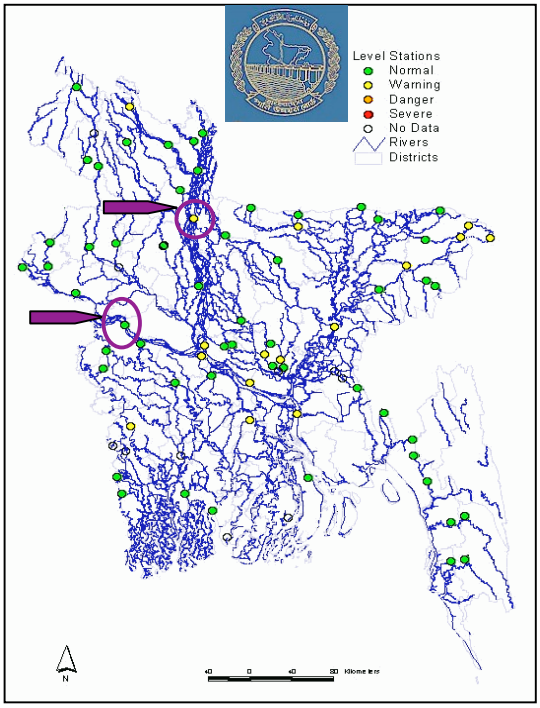

Fig. 5 – Bangladesh Flood Forecasting and Warning Center water level gauge network.

This graphic shows the flood danger status as of 31 July 2006.

Observational discharge data for the years 2001 and 2002 come from the two stations highlighted by purple arrows and circles: Bahadurabad (above right) and Hardinge Bridge (below left).

[4] Dr Peter Webster's CFAB web page available online at: http://cfab.eas.gatech.edu/cfab/cfab.html

[5] Bangladesh Flood Forecasting and Warning Center: http://www.ffwc.gov.bd/

7. Ganges/Brahmaputra Results

Table 1 shows the No Routing Case results of LIS NOAH land surface model generated values for surface runoff (Qs), subsurface baseflow (Qsb), and total flow (Qtot) for 2001 (left) and 2002 (right). All values are in m^3/s and rounded to the nearest 10 for uniform comparison.

Month	Qs	Qsb	**Qtot**	Qs	Qsb	**Qtot**
Jan	150	1,710	**1,860**	90	2,910	**3,000**
Feb	40	1,770	**1,810**	340	1,590	**1,930**
Mar	90	880	**970**	150	980	**1,130**
Apr	960	1,640	**2,600**	570	2,030	**2,600**
May	1,180	2,520	**3,700**	1,270	3,860	**5,130**
Jun	6,230	11,130	**17,360**	5,100	10,630	**15,730**
Jul	7,160	25,510	**32,760**	2,270	17,340	**19,610**
Aug	4,080	35,670	**39,750**	7,250	37,240	**44,490**
Sep	1,850	18,680	**20,530**	3,440	41,500	**44,940**
Oct	2,130	17,330	**19,460**	2,470	23,060	**25,530**
Nov	390	9,980	**10,370**	530	20,320	**20,850**
Dec	260	4,090	**4,350**	130	7,590	**7,720**

Table 2 shows the GRDC climatological values – Farakka (1949-1973) + Bahadurabad (1969-1992) extreme minimum, mean, and extreme maximum.

Month	GRDC min	GRDC mean	GRDC max
Jan	6,150	7,900	11,240
Feb	5,000	6,580	9,070
Mar	4,800	6,940	9,550
Apr	7,500	10,160	13,600
May	8,890	17,510	30,780
Jun	19,300	36,130	55,050
Jul	43,990	69,900	93,250
Aug	49,400	88,050	120,930
Sep	49,830	79,840	105,130
Oct	22,130	46,280	76,240
Nov	12,460	19,090	29,120
Dec	8,080	11,200	14,860

At first glance the values from Qtot look low compared with the range given by the GRDC climatology, finally approaching the GRDC extreme minimum in August and September (within 10%) then staying within range from October to December (within 5%). From this table we can see the relative contributions of the surface runoff as an integrator of the rainfall over the area versus the subsurface baseflow acting as slower responding integrator of soil moisture. In the dry winter months the surface runoff makes up only a small portion of the total river discharge, then as the summer monsoon begins in June the impact of the rainfall can be seen making up almost 50% of the total discharge. By July the subsurface baseflow starts to jump dramatically as the soil moisture retains memory of the earlier rainfall. It is interesting to see that there is little difference between the August and September LIS generated total discharge (without routing), but that the contribution from Qs and Qsb has changed.

Overall, we find that the LIS generated discharge from surface runoff, Qs, alone without using river routing does not make a good choice as an estimate for the total river discharge.

The LIS generated discharge from the subsurface baseflow, Qsb, would make a better fit to the climatology values given the relative size of this term compared to the Qs term. Using the combination of both Qs and Qsb generated over a basin wide area and averaged for each month could give an acceptable estimate for river discharge for un-gauged areas where no real-time observations are available provided that the model used had been adequately “spun-up”.

Table 3 shows the Vic Routing Case results of LIS Qs and Qsb that have been routed along the STN-30 river network. We compare these values against the observations for Hardinge Bridge (acting as Farakka) + Bahadurabad (column 2 & 5). Output values are given for the STN-30 stations Farakka + Bahadurabad (column 3 & 6) and the STN-30 Ganges-Brahmaputra Outlet (column 4 & 7). All values are in m^3/s and rounded to the nearest 10 for uniform comparison. Results are for 2001 (left) and 2002 (right).

Month	F+B Obs	F+B VIC	GB VIC	F+B Obs	F+B VIC	GB VIC
Jan	6,060	1,220	1,630	7,080	1,540	1,860
Feb	4,870	690	910	6,230	1,170	1,460
Mar	4,300	570	780	5,740	880	1,040
Apr	5,690	640	690	9,150	1,490	1,960
May	9,960	3,700	6,190	14,160	6,330	8,840
Jun	27,120	12,130	21,440	27,580	15,230	22,240
Jul	52,320	15,330	23,550	66,190	28,040	39,080
Aug	78,430	35,940	41,380	74,060	38,120	49,760
Sep	77,250	44,040	46,590	48,600	42,470	45,360
Oct	46,150	21,170	32,510	32,830	33,230	46,910
Nov	17,190	6,060	10,510	14,600	9,440	13,530
Dec	10,270	2,280	3,310	9,650	4,360	6,220

Information contained in Tables 4.1 – 4.3 are also presented in Figure 6.

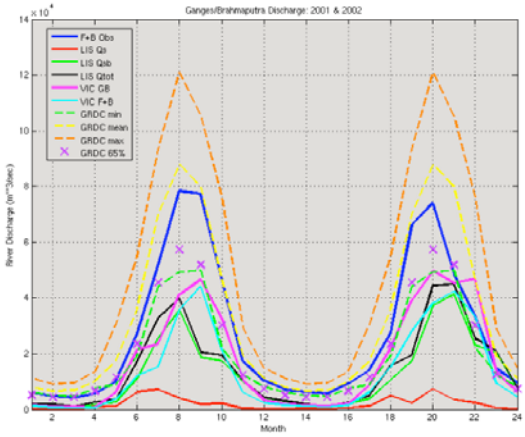

Fig. 6 – Ganges/Brahmaputra Monthly River Discharge – 2001 to 2002. Observations from Hardinge Bridge + Bahadurabad, Bangladesh (shown as F+B Obs, blue); No routing GB basin wide values for LIS surface runoff, Qs (red), LIS subsurface baseflow, Qsb (green), and LIS Qtot (black); VIC routing cases with totals for values at the STN-30 Farakka and Bahadurabad station locations (cyan) and for the STN-30 GB outlet (magenta). GRDC station climatology (Farakka, India + Bahadurabad) are included for comparison: extreme minimum (green --), mean (yellow --), extreme maximum (orange --), and 65% of the mean (purple x).

When we look at the results using the VIC river routing model we see that the dry season months are somewhat lower than the observed GRDC extreme minimums, but that the peak of the monsoon is close to their corresponding GRDC extreme minimum values. Without knowing more about the monsoon for the 2002 calendar year and without having access to the latest river discharge observations from these GRDC stations it would be difficult to make an immediate assessment on the impact of river routing.

So if the only river data we had were from the GRDC climatology we would need to first see if the low values were consistent with an abnormally dry monsoon for 2002. Upon checking the Monsoon On-line website[6] produced by the Indian Institute for Tropical Meteorology one finds out that 2002 was indeed a drought year (sixth driest in 130 years) with rainfall being ~35% less than normal by mid-August (Figure 7), recovering somewhat by the end of the monsoon.

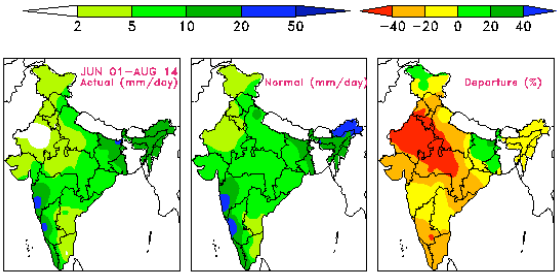

Fig. 7 Cumulative Rainfall for Monsoon 2002 for the period June 01 to August 14.
Source – the Indian Institute of Tropical Meteorology.

If we multiply the GRDC mean values for the summer monsoon months by 0.65, we end up with values that do indeed resemble the VIC routing values and the GRDC observed climatological minimums (see Figure 6).

However, thanks to the CFAB group at GT daily river discharge data is available for the year 2002. Of course, these data are not measured at the Ganges/Brahmaputra outlet and do not include the contribution of any surface runoff generated due to rainfall over Bangladesh. In Jun Jian's Master's Thesis (2005), he states that it has been estimated that only 10-15% of the rainfall over Bangladesh itself contributes to the river flow in the delta.

[6] Monsoon On-line website - http://www.tropmet.res.in/%7Ekolli/MOL/

The results presented here show a difference between the VIC routing modeled at the STN-30 Farakka and Bahadurabad stations and the VIC routing modeled at the Ganges/Brahmaputra outlet between 6% (September) and 31% (June) with an average difference of 23%. We can probably account for these differences by considering the contributing subsurface baseflow of the Meghna River which is modeled in the STN-30 network as a smaller branch within the GB basin located south of the Farakka and Bahadurabad STN stations (marked by a yellow circle in Figure 4).

When we compare the VIC routing results to the FFWC observations we see that the peak August value is much higher than the GRDC minimum but still less than the GRDC mean.

In Figures 8 and 9 we compare the performance of the routing and no routing cases on a daily basis. In general, both VIC routing results follow the FFWC observations in their pattern, but miss the extreme peaks of July and August 2001as well as August 2002.

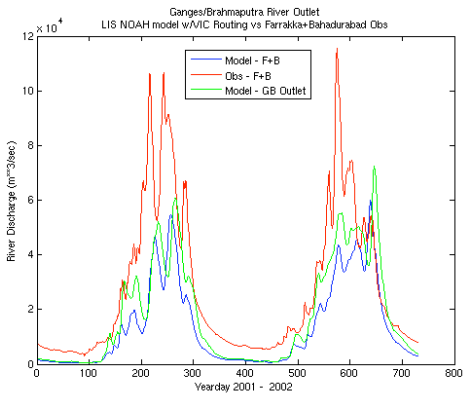

Fig. 8 VIC routing cases 2001 - 2002. Observations from Hardinge Bridge + Bahadurabad, Bangladesh (shown as Obs – F+B, red); and VIC routing cases with totals for values at the STN-30 Farakka and Bahadurabad station locations (blue) and for the STN-30 GB outlet (green).

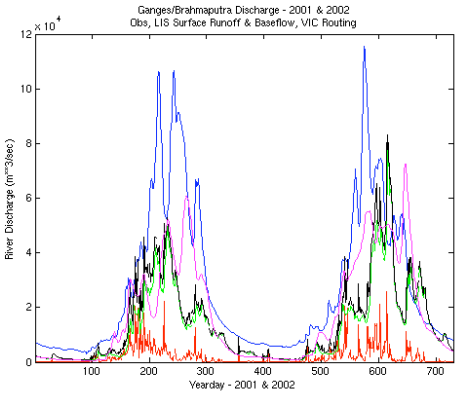

Fig. 9 No routing case 2001 - 2002. Observations from Hardinge Bridge + Bahadurabad, Bangladesh (shown as F+B obs, blue); No routing GB basin wide values for LIS surface runoff, Qs (red), LIS subsurface baseflow, Qsb (green), and LIS Qs + Qsb (black). VIC routing for the STN-30 GB outlet (magenta) added for comparison.

The GB VIC routing misses a minor peak in late May and shows a delayed peak occurring in early October. The F+B VIC routing matches this peak with the FFWC observations, finally catching up by end of September. These results reflect the findings by Webster and Hoyos (2004) of three important characteristics of the south Asian monsoon. First, the mean seasonal cycle is smooth, with rainfall staring in late May, reaching a maximum in July, and then slowly decreasing through September. Second, the rainfall distribution in any one year is made up of a series low frequency sequences of rainy periods (“active” periods) with intervening dry periods (monsoon “breaks”) each lasting 10-30 days. Third, the smoothness of the mean annual cycle of precipitation suggests that there is no preferred time for the large-amplitude active and break periods of the monsoon to occur.

Indeed, the magnitude of the intra-seasonal variability has been shown to be far greater than the inter-annual variability (e.g. Webster and Hoyos, 2004; Webster et al. 1998; Waliser et al. 1999). Thus, for a 0.25° × 0.25° resolution LSM forced by satellite-derived precipitation and numerical weather model atmospheric data, then routed on a 0.5° × 0.5° artificial river network, the overall results are encouraging.

One possible explanation for the lower than expected VIC routing values for the dry, winter months (Jan-Apr) is a problem encountered when using a post-processor river routing model. Because the LIS model state file contains only information about the state variables that are internal to the LIS model, it does not store information about the routing process. As a result, the routed runoff from a LIS model run that is restarted from a state file is under-predicted compared to a LIS model run that has been "properly" spun-up (for example by throwing away the first × number of years of simulation). According to the VIC online documentation this start-up effect will disappear after a few months (depending on the travel time in the routing network), when the routing arrays are properly "filled". Conceptually the problem is that the river channels are started "empty" because no state file is stored for the routing arrays.

The suggested solution is to use the runoff file (input to the routing model) from a base run (the one that produced the state file) to extend the restarted run backwards into time. The amount of extension going backwards into time depends also on the travel time in the routing network, but that "two or three months" should be sufficient.

This should "fill the channels" and the routed flows of the model runs will be the same as a longer, continuous run. Since the signal of interest falls in the summer monsoon months this start-up effect can be acknowledged, but not necessarily corrected for.

All the results presented here have been corrected for this "fill the channels" problem. The low values at the start of the year do indeed catch-up within 2 months. At the Ganges/Brahmaputra outlet, for both 2001 and 2002, the date when the corrected and uncorrected values match is February 26.

8. Results for Other Basins

Table 4 (a) Irrawaddy Basin – GRDC Station Sagaing Climatology (1978-1988), VIC routing at STN-30 station Sagaing for 2001 (column 4) and 2002 (column 5).

Month	GRDC min	GRDC mean	GRDC max	VIC Sagaing	VIC Sagaing
Jan	1,820	2,530	3,090	60	40
Feb	1,350	1,920	2,550	30	40
Mar	1,420	2,420	3,740	20	30
Apr	2,000	3,450	4,900	40	30
May	2,750	4,340	6,370	70	110
Jun	4,130	9,010	16,410	540	210
Jul	11,630	16,410	21,090	1,190	2,170
Aug	13,420	17,620	20,270	2,150	4,290
Sep	12,370	17,160	24,780	2,130	2,040
Oct	7,840	12,780	16,590	1,260	920
Nov	3,440	5,230	7,220	1,150	470
Dec	2,830	3,440	4,410	220	150

Table 5 Godavari Basin – GRDC Station Polavaram Climatology (1901-1979), VIC routing at STN-30 station Polavaram (~ same as STN-30 Godavari outlet) for 2001 (column 4) and 2002 (column 5).

Month	GRDC min	GRDC mean	GRDC max	VIC Polavaram	VIC Polavaram
Jan	30	250	460	150	190
Feb	70	200	540	80	100
Mar	60	150	420	90	70
Apr	30	120	700	150	90
May	10	90	290	120	170
Jun	40	970	7,580	740	610
Jul	190	7,600	34,610	1,900	2,180
Aug	2,310	11,570	26,480	1,910	3,620
Sep	1,790	10,120	32,730	2,040	12,160
Oct	730	3,890	14,990	1,940	3,030
Nov	230	1,070	4,140	770	1,170
Dec	140	420	1,800	210	350

Table 4.6 Krishna Basin – GRDC Station Vijayawada Climatology (1901-1979), VIC routing at STN-30 station Vijayawada (~same as STN-30 Krishna outlet) for 2001 (column 4) and 2002 (column 5).

Month	GRDC min	GRDC mean	GRDC max	VIC Vijay.	VIC Vijay.
Jan	0	110	640	230	350
Feb	0	60	310	150	190
Mar	0	50	660	120	130
Apr	0	30	200	180	110
May	0	120	1,060	110	240
Jun	10	500	1,740	320	440
Jul	60	4,710	12,250	1,190	1,420
Aug	210	6,270	16,560	1,210	2,080
Sep	550	4,080	9,220	680	3,580
Oct	200	2,600	6,560	2,690	3,060
Nov	0	940	9,460	1,990	3,860
Dec	0	240	1,070	420	930

Table 4.7 Salween Basin – VIC routing at STN-30 Salween outlet for 2001 (column 2) and 2002 (column 3). There are no GRDC stations available for climatology.

Month	VIC Salween Outlet	VIC Salween Outlet
Jan	120	140
Feb	60	100
Mar	60	70
Apr	40	60
May	70	160
Jun	210	220
Jul	340	1,420
Aug	1,560	3,940
Sep	1,250	7,120
Oct	1,700	2,630
Nov	980	1,150
Dec	310	510

9. Discussion and Conclusions

Looking at the results for the other basins, we see that for the Irrawaddy basin the LIS model run using VIC river routing greatly underestimates the monthly discharge totals – even the GRDC extreme minimums. This could be evidence of the "start-up effect" mentioned above, poor CMAP precipitation forcing fields, or that the GRDC climatology (1978-1988) does not reflect the true range of variability experienced this particular river system.

On the other hand, the results for the Godavari and Krishna basins are encouraging. Both have river gauge stations with a long time series (1901-1979) for establishing credible minimum, mean, and maximum values. Both of these river gauge stations (Polavaram – Godavari, Vijawada – Krishna) are located at or near the river outlet (at least in terms of a 0.5° network) so a good comparison can be made between the model output and observations.

Unfortunately, public access to latest real-time river discharge observations is next to impossible. One possible reason for this is that water resources are an important political issue within the individual provinces of India adding to the difficulties of reporting and sharing data (Ajoy Kumar, pers. comm. 2006).

Finally, results are shown for the estimated river discharge from the Salween basin. No GRDC stations are available on this river system, so no direct comparison can be made. Judging by the poor performance of the model run in describing the Irrawaddy basin, we believe that the Salween is also greatly underestimated. But this points out the main potential benefit of having a land surface model connected to a river routing model forced by satellite-derived precipitation – getting a river discharge estimate for an un-gauged river in a data sparse area.

One of the main features of the VIC river routing code is the ability to get estimates for any location within a river network. So one can make comparisons to known river gauge station observations, even if those stations are located far upstream from the river outlet to the ocean. Results for those cases are not shown here given the lower volume rates involved.

Appendix

We can determine whether a river routing model is required to direct the flow of surface runoff to the ocean given a monthly time scale. Using the University of New Hampshire's STN-30 river network and the STN-30 data file listing the length to the each river's ocean outlet for every 0.5° grid contained in the area of interest, we can calculate a general velocity based on the slope at each point using the equations and parameters presented in the classic textbook, *Applied Hydrology* (Chow, Maidment and Mays, 1988). With the distance and velocity we can calculate the time it takes for water to flow to its respective river outlet in the Bay of Bengal.

To derive the slope for each point of the network, we used the high resolution (2 min) ETOPO2 digital elevation model (DEM) obtained from the National Oceanic and Atmospheric Administration (NOAA) National Geophysical Data Center (NGDC). The slope calculation for each grid point follows the method used within ESRI's Geospatial Information System (GIS) software ArcView. The "King's Case" algorithm calculates the slope for a center grid cell using all 8 surrounding grid cells as follows:

A	B	C
D	E	F
G	H	I

"King's Case"

Slope = Rise over Run, equivalent to tangent of slope angle. X-grid, Y-grid spacing ~ 4 km

$$\text{Slope} = \tan \beta = [(\Delta z/\Delta x)^2 + (\Delta z/\Delta y)^2]^{1/2} * 100\% \quad (5)$$

$$(\Delta z/\Delta x)^2 = \{[(A + 2D + G) - (C + 2F + I)] \div (8 * \text{x-grid spacing})\}^2 \quad (6)$$

$$(\Delta z/\Delta y)^2 = \{[(A + 2B + C) - (G + 2H + I)] \div (8 * \text{y-grid spacing})\}^2 \quad (7)$$

This basic algorithm is adjusted for grid points that are located on the corners and borders of the study region (not shown).

Once the slopes have been calculated, river flow velocities (Table A) can be derived based on the groupings found in the textbook, *Applied Hydrology* (Chow, Maidment and Mays, 1988).

Table A River flow velocities (in m/sec) dependent upon on the steepness of the slope and land use category.

	Slope 0-3%	Slope 4-7%	Slope 8-11%	Slope 12% +
Unconcentrated				
Landcover: Woodlands	0 – 0.46	0.46 – 0.76	0.76 – 1.00	1.00 +
Landcover: Pastures	0 – 0.08	0.76 – 1.07	1.07 – 1.30	1.30 +
Landcover: Cultivated	0 – 0.91	0.91 – 1.37	1.37 – 1.68	1.68+
Landcover: Rocky/Paved	0 – 2.59	2.59 – 4.11	4.11 – 5.18	5.18 +
Concentrated				
Natural Channel	0 – 0.61	0.61 – 1.22	1.22 – 2.13	2.13 +

Based on this table the following values were chosen: 0-3% 0.61 m/sec, 4-7% 0.91 m/sec, 8-11% 1.3 m/sec, and 12% 1.6 m/sec. The slope values calculated for the study area are shown in Figure A.1.

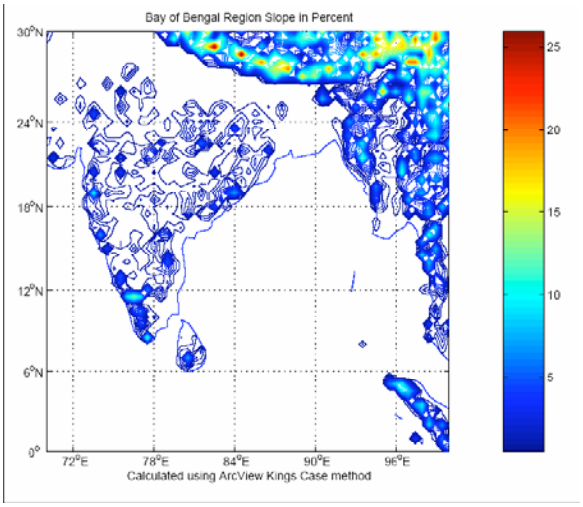

Fig. A.1 – The slope values calculated using ArcView King's Case method. One can see that the highest slope values are limited to the Himalaya's (slopes > 12%) and are very flat in the Gangetic Plain (slopes < 1%).

One can see that the highest slope values are limited to the Himalaya's (slopes > 12%) and are very flat in the Gangetic Plain (slopes < 1%). The resulting velocities (converted into m/sec) are shown in Figure A.2

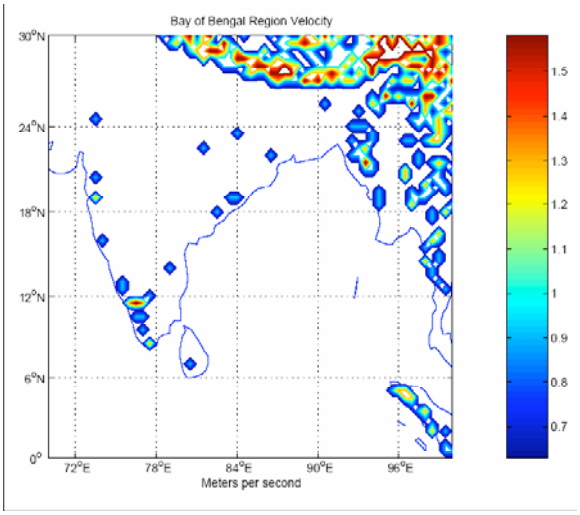

Fig. A.2 – The velocity values are derived based on the groupings found in Table A.

Some of the longer distances in the STN-30p data file are between 2000 km and 3000 km with a few reaching close to 3500 km (results not shown). Travel times equaled one month or less for most of the study area except for the headwaters of the Ganges River (30-40 days) and Brahmaputra River (50-60 days) (Figure A.3).

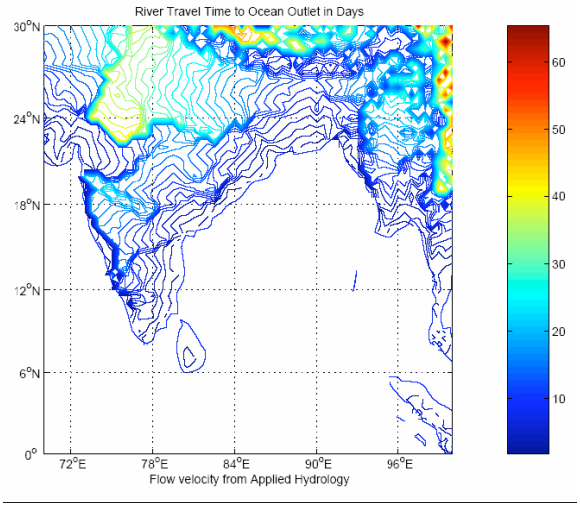

Fig. A.3 – The travel time values are derived from the previously determined velocity and the distance to ocean outlet values from the University of New Hampshire STN-30 network.

These values are in line with those quoted by Oki and Sud (1998):

"The traveling time for 1500 km is of the order of 2 weeks, if the flow velocity in the streams is of the order of 1 m/sec. The error in estimating traveling time, caused by the poor reproduction of stream length, can be in the 10%–25% range if such errors appear randomly. Its effect could be neglected, particularly for monthly water balance studies, but it could be crucial for flood forecasting."

Acknowledgement

This work was conducted under sponsorship by NASA Earth System Science Fellowship, ESSF-03-000-0053.

Many thanks go to the author's advisor, Dr Peter J Minnett and the NASA GSFC LIS project team directed by Dr Christa Peters-Lidard.

References

Bosilovich, M.G., R. Yang, P.R. Houser (1999). River basin hydrology in a global off-line land-surface model. *Journal of Geophysical Research*, **104**(D16), 19661-19673.

Chorowicz, J., C. Ichoku, S. Riazanoff, Y.-J. Kim, and B. Cervelle (1992). A combined algorithm for automated drainage network extraction. *Water Resources,* **28**, 1293–1302.

Chow, V.T., Maidment D.R., and Mays L.W. (1988). *Applied Hydrology*. McGraw-Hill Book Co, New York, 572 pp.

Costa-Cabral, M.C. and S. J. Burges (1994). Digital elevation model networks (DAEMON): A model of flow over hillslopes for computation of contributing and dispersal areas. *Water Resources,* **30**, 1681–1692.

Ek, M., K. Mitchell, L. Yin, P. Rogers, P. Grunmann, V. Koren, G. Gayno, and J. Tarpley (2003). Implementation of Noah land-surface model advances in the NCEP operational mesoscale Eta model. *Journal of Geophysical Research*, **108**(D22), 8851-8866.

Fekete, B.M., C.J. Vörösmarty, and W. Grabs (2000). Global, composite runoff fields based on observed river discharge and simulated water balances. Online at: http://www.grdc.sr.unh.edu/

Fread, D.L. (1993). Flow Routing. In; *Handbook of Hydrology*, Ch. 10, D.R. Maidment (ed.) McGraw Hill.

Jian, J. (2005). Master's Thesis – Relationship between the Pacific Ocean SST Variability and the Ganges-Brahmaputra River Discharge. Georgia Institute of Technology, 55 pp.

Kumar, S.V., C.D. Peters-Lidard, Y. Tian, P.R. Houser, J. Geiger, S. Olden, L.Lightly, J.L. Eastman, B. Doty, P. Dirmeyer, J. Adams, K. Mitchell, E.F. Wood, and J. Sheffield (2006). Land Information System - An Interoperable Framework for High Resolution Land Surface Modeling. *Submitted to Environmental Modelling & Software.* Online at: http://lis.gsfc.nasa.gov/Papers/index.shtml.

Lau, K.M., J.H. Kim, and Y. Sud (1996). Intercomparison of Hydrologic Processes in AMIP GCMs. *Bulletin of the American Meteorology Society*, **77**(10), 2209-2227.

Lohmann, D., R. Nolte-Holube, and E. Raschke (1996). A large-scale horizontal routing model to be coupled to land surface parameterization schemes, *Tellus*, **48A**,5, pp708-721.

Lohmann, D., E. Raschke, B. Nijssen, and D. P. Lettenmaier (1998a). Regional Scale Hydrology: I. Formulation of the VIC-2L Model Coupled to a Routing Model, *Hydrological Sciences Journal*, **43(1)**, pp 131-141.

Lohmann, D., E. Raschke, B. Nijssen, and D. P. Lettenmaier (1998b). Regional Scale Hydrology: II. Application of the VIC-2L Model to the Weser River, Germany, *Hydrological Sciences Journal*, **43(1)**, pp 143-157.

Mesa, O.J. and E.R. Mifflin (1986). On the relative role of hillslope and network geometry in hydrologic response. In: V.K. Gupta, I. Rodriguez-Iturbe and E.F. Wood (eds). *Scale problems in Hydrology*, pp 1-17.

Miller, J.R., G.L. Russell, G. Caliri (1994). Continental-Scale River Flow in Climate Models. *Journal of Climate*, **7**, 914-928.

Oki, T. and Y. Sud (1998). Design of Total Runoff Integrating Pathways (TRIP)-A Global River Channel Network. *Earth Interactions*, **2**, 1-36.

Pfaendtner, J., S. Bloom, D. Lamich, M. Seablom, M. Sienkiewicz, J. Stobie, and A. daSilva (1995). Documentation of the Goddard Earth Observing System (GEOS) Data Assimilation System - Version 1, NASA Technical Memorandum 104606, 4, 44 pp.

Prasanna Kumar, S., P.M. Muraleedharan, T.G. Prasad, M. Gauns, N. Ramaiah, S.N. de Souza, S. Sardesai, and M. Madhupratap (2002). Why is the Bay of Bengal less productive during summer monsoon compared to the Arabian Sea. *Geophysical Research Letters*, **29**(24), 2235.

Reynolds, C., T. Jackson, and W. Rawls (1999). Estimating available water content by linking the FAO soil map of the world with global soil profile database and pedo-transfer functions. In American Geophysical Union Fall Meeting, *EOS Transactions*, page 80.

Rodell M., P.R. Houser, U. Jambor, J. Gottschalck, K. Mitchell, C.-J. Meng, K. Arsenault, B. Cosgrove, J. Radakovich, M. Bosilovich, J. K. Entin, J. P. Walker, D. Lohmann, and D. Toll (2004). The global land data assimilation system. *Bull. Amer. Met. Soc.*, **85**, 381-394.

Rodell, M., P.R. Houser, A. Berg, and J.S. Famiglietti (2005). Evaluation of 10 Methods for Initializing a Land Surface Model. *Journal of Hydrometeorology*, **6**(2), 146-155.

Strahler, A.N. (1964). Quantitative geomorphology of drainage basins and channel networks. In: V.T. Chow (ed). *Handbook of Applied Hydrology*. McGraw Hill.

Tomczak, M. and J.S. Godfrey (1994). *Regional Oceanography: An Introduction*. Pergamon, 422 pp.

VIC operation overview (2002). Online at: http://www.hydro.washington.edu/Lettenmaier/Models/VIC/Documentation/test_oper.html.

Vörösmarty, C.J., B.M. Fekete, M. Meybeck and R.B. Lammers (2000). Global system of rivers: Its role in organizing continental land mass and defining land-to-ocean linkages, *Global Biogeochemical Cycles*, **14(2)**, 599-621.

Waliser, D.E., C.E. Jones, J.K. Schemm, and N.E. Graham (1999). A statistical extended-range tropical forecast model based on the slow evolution of the Madden-Julian oscillation. *Journal of Climate*, **12**, 1918-1939.

Webster, P.J. and C. Hoyos (2004). Prediction of Monsoon Rainfall and River Discharge on 15-30-Day Time Scales. *Bulletin of the American Meteorological Society*, **85**(11), 1745-1765.

Xie P., and P.A. Arkin (1996). Global precipitation: a 17-year monthly analysis based on gauge observations, satellite estimates, and numerical model outputs. *Bulletin of the American Meteorological Society*, **78**, 2539-2558.

Yang, Z.-L., R.E. Dickinson, A. Henderson-Sellers, and A.J. Pitman (1995). Preliminary study of spin-up processes in land surface models with the first stage data of Project for Inter-comparison of Land Surface Parameterization Schemes Phase 1(a). *Journal of Geophysical Research*, **Vol. 100**, **D8**, 16533-16578.